Indian Journal of Chemical Technology
Vol. 23, September 2016, pp. 384-391

Oxidative carbonylation of methanol to dimethyl carbonate over Cu/AC catalysts prepared by microwave irradiation: Effect of La and Zr promoters

Yongli Pei[1], Jinzhou Yang[1], Meijiao Ren[1], Wei Wang[1], Jun Ren*,[1], Jianying Lin[1,2] & Zhong Li[1,2]

[1]Key Laboratory of Coal Science and Technology (Taiyuan University of Technology),
Ministry of Education and Shanxi Province, 030024 Taiyuan, China

[2]No. 79 Yingze West Street, Taiyuan 030024, China

E-mail: renjun@tyut.edu.cn

Received 10 May 2014; accepted 13 September 2015

Copper catalysts with a loading of 16.7 wt%, supported on activated carbon (AC) with the addtion of La or Zr, have been prepared by microwave heating methods and tested for the oxidative carbonylation of methanol to dimethyl carbonate (DMC). X-ray diffraction (XRD, temperature-programmed reduction (TPR), XPS), and scanning electron micrographs (SEM) have been carried out to examine the bulk and surface properties of the carbon-supported copper catalysts. It is found that the addition of La or Zr promoters favours the auto-reduction of copper precursors to metallic copper and leads to smaller and even nanoparticle-size Cu distributed on the surface of the carbon support which exhibt promising space-time yield of DMC of 480.2 and 585.2 $mg \cdot g^{-1} \cdot h^{-1}$, respectively. Meanwhile, the selectivity of DMC reached 95.7 and 90.3% and higher conversion of CH_3OH of approximately 4.0 and 4.7% have been achieved surprisingly, even after five sets of relevant experiments. The improved catalytic performance of Cu/AC with the addition of La or Zr in the DMC synthesis is due to the presence of more metallic copper, more evenly distributed over the surface of the carbon support, with a significantly reduced particle size as compared with no La or Zr promoter.

Keywords: Dimethyl carbonate (DMC), Microwave heating, Cu/AC catalysts, Cu nanoparticle, Promoters

Dimethyl carbonate (DMC) is an environmentally benign chemical compound and a unique intermediate with versatile chemical reactivity. It has attracted increasing interest from both practical and theoretical points of view over recent years. The one-step liquid-phase methanol oxidative carbonylation process, developed by Enichem, is by far the most popular phosgene-free route for the industrial production of DMC. However, this process produces severe equipment corrosion and catalyst deactivation because CuCl has been used as the active catalysts[1].

In recent years, a great deal of interest has focused on vapor-phase oxidative carbonylation of methanol because it has been found to be almost free from corrosion[2]. However, Cu (II) chloride-based catalysts such as $CuCl_2$, $CuCl_2$-$PdCl_2$ or $CuCl_2$ promoted by acetates or hydroxides suffered from a strong deactivation due to the loss of the chloride involved in the reaction[3–6]. Yuan *et al.*[7] reported that amino functionalization can improve the activity and stability of $CuCl_2$/MCM–41 and $CuCl_2$/MCM–48 catalysts in the synthesis of DMC. King[8] showed that Cu-exchanged Y zeolite catalysts, prepared by a solid-state ion exchange method (SSIE), displayed good productivity and selectivity for DMC synthesis with a strongly enhanced stability compared with the usual activated charcoal supported chloride-based catalysts. Various Cu-exchanged zeolites obtained by this method, such as Cu-MCM–41 (Ref 9), Cu-X (Ref 10), Cu-ZSM-5 (Ref 11), as well as Cu/β (Ref 12), have been extensively investigated as potential candidates for vapour-phase DMC synthesis. Bell and his co-workers performed a detailed experimental and theoretical investigation on the mechanisms of DMC synthesis on Cu-Y[13,14]. Richter *et al.*[15,16] found that incipient wetness impregnation of zeolite Y with copper(II) nitrate solution and inert activation at 650°C could lead to chloride-free Cu-zeolite catalysts for the synthesis of DMC.

Recently, Li and co-workers prepared chlorine-free Cu_2O/AC catalysts by impregnating activated carbon with copper acetate followed by heat treatment in an inert atmosphere. It was found that the treatment of the AC with nitric acid or ammonia favored the reduction of Cu^{2+} to Cu^{1+} and improved the dispersion of the Cu species and the catalytic activity[17]. Furthermore, Li and co-workers found that heat treatment of AC impregnated with cupric nitrate at

different temperatures can produce CuO, Cu_2O and Cu^0 catalysts. It appeared that these copper species are active for the oxidative carbonylation of methanol, and the catalytic activity increased in the order $CuO<Cu_2O<Cu^0$ (Ref 18). Pd-doped zeolites[19,20] were recently studied in the DMC synthesis. It was found that the Pd species were maintained in an electron-deficient state as the active species for the reaction and the Lewis acidic sites in the zeolites promote the catalytic performance of the Pd-doped zeolites.

In our previous studies, the highly dispersed Cu/C catalysts were prepared by using $Cu(NO_3)_2$ and starch as primary source materials and used for the DMC synthesis[21]. A detailed study on the mechanism of DMC formation on Cu^0/AC catalysts was performed with the DFT method and the main pathway of DMC formation is presented. The calculated results provided the evidence for the high activity of Cu^0/AC catalysts in oxidative carbonylation of methanol[22]. In addition, a functional yolk–shell nanoparticles (YSNs) within a hollow porous carbon shell were successfully synthesized (Cu@Carbon) which exhibited the excellent thermal stability and promising catalytic properties toward DMC synthesis[23].

It is well known that the catalytic activity strongly depends on the size and size distribution of the metal particles and their dispersion on the support[24]. Therefore, metal particles with high electrocatalytic activity need to be of a suitable size with a narrow size distribution. However, conventional preparation techniques based on wet impregnation and the chemical reduction of metal precursors do not provide satisfactory control of particle shape and size[24]. The synthesis of highly dispersed supported Cu particles, whose size is controlled and uniform, still remains a challenge.

Recently, the preparation of catalysts by microwave irradiation has been developed as an effective technique in our team, where carbon powder with high surface area, mixed with aqueous solutions of copper and other salts, acts both as a microwave energy susceptor and support to produce carbon-supported copper catalysts[25,26]. Meanwhile, the decomposition process of copper nitrate under microwave irradiation has been investigated in detail[27]. Microwave synthesis is generally considered to be rapid and very energy efficient. Reactions occur at lower temperatures and in a much shorter time in microwave synthesis than in conventional methods. Microwave synthesis has produced products with good phase purity, a high degree of crystallinity and particle sizes on the nanoscale[28-32]. As well as small particles with large surface area, crystallites can also be prepared that are bigger than those obtained using conventional methods. The effect of microwaves varies greatly from material to material. Activated carbon powders are known to absorb microwaves very rapidly[33].

Copper-based catalysts such as Cu/ZrO_2 (Ref 34-36), Cu-Zn[37] and Cu-Zn-Al[38,39] have often been used for the synthesis of methanol and dimethyl ether (DME). It has been found that the addition of La[34-36] and Zr[37-39] can greatly improve the dispersion of the copper on the surface of these catalysts. In the present work, the influence of La and Zr promoters on the catalytic performance of the Cu/AC catalysts in the DMC synthesis has been investigated. The prepared samples were characterized by XRD, SEM, TPR and XPS measurements to establish a fundamental understanding of the relationship between the catalytic performance and the nature of the active sites in the carbon-supported copper catalysts.

Experimental Section

Catalyst preparation

The activated carbon used in this work is a commercial product from Xinhua Chemical Plant (Taiyuan, China), which was crushed into particles of 40-60 mesh (0.3-0.45 mm) before use. The AC has a specific surface area of 864 m^2/g, a micro-pore volume of 0.22 mL/g and a meso-pore volume of 0.27 mL/g. The Cu/AC catalysts were prepared by the impregnation method. A typical procedure is as follows: 3.2 g AC was impregnated with a solution of 2.44 g of $Cu(NO_3)_2 \cdot 3H_2O$ and 0.3 g of $La(NO_3) \cdot 6H_2O$ (or 0.3 g of $Zr(NO_3)_4 \cdot 5H_2O$) dissolved in 10 mL of deionized water at 70°C for 12 h. Water was removed by heating, and drying was carried out at 90°C for 12 h. The loading of Cu was 16.7 wt%, and the La (or Zr)/Cu mole ratio is 0.15%. The samples were mixed with quartz grain (40-60 mesh) with a weight ratio of 1:1.5, then subjected to microwave heating in a microwave experimental setup (Jiequan NJZ4-3, 2.45 GHz, 0-4.2 kW). The heating of the powder mixture was carried out in an alumina crucible in a vacuum of –0.05 MPa. The sample temperature was ramped to 350°C at a rate of 0.4-0.6°C/s with output power of 0.05~0.6 kW, and then cooled down to RT. The dried mixtures were sieved through a 0.8 mm

screen. The samples were denoted Cu/AC, LaCu/AC and ZrCu/AC.

Characterization technique and procedures

X-ray diffraction (XRD) data were recorded on a Rigaku D/max 2500 diffractometer using CuK_α radiation (40 kV and 100 mA) over a 2θ range of 10°–80° at a *scanning rate* of 1°/min.

Temperature-programmed reduction (TPR) measurements were performed with a Finsore-3010 chemisorption analyzer (Finetec Instruments) equipped with a TCD for monitoring the H_2 consumption from a feed stream containing 10 vol% H_2 in Ar. In these experiments, 50 mg of catalyst were loaded in the reactor which was then purged with pure Ar. The temperature was then ramped from room temperature to 200°C with a heating rate of 10 K min^{-1} and held for 1 h. The temperature was then reduced to 50°C, the reducing mixture was introduced at 20 ml/min, and heating was started using a 10°C/min gradient to 500°C. The consumption of H_2 was determined using a thermal conductivity cell. TPR measurements were taken from 50 to 500°C with a heating rate of 10 K min^{-1}.

X-ray photoelectron spectroscopy (XPS) data were collected on an ESCALab220i-XL electron spectrometer (VG, UK) using 300 W AlK_a radiation. The samples were compressed into a pellet 2 mm thick and then mounted on a sample holder using double-sided adhesive tape. The sample holder was then placed in a fast entry air load-lock chamber without exposure to air and evacuated ($<10^{-6}$ Torr) overnight. Finally, the sample holder was transferred to the analysis chamber for XPS study. The base pressure inside the analysis chamber was usually maintained at better than 10^{-10} Torr. The binding energies were referenced to the C1s line at 284.6 eV *from* adventitious carbon. Curve deconvolution of the XP spectra was performed using the XPS Peak Fitting Program (XPSPEAK41, Chemistry, CUHK).

Scanning electron micrographs (SEM) were obtained with a JEOL-JSM-6701F instrument able to give magnifications of 100000. The tungsten wire was saturated with a 3 A current and the electrons were accelerated with a ddp of 20 kV. The samples were coated with gold, and micrographs of the particles were taken with a Polaroid camera. The final catalyst composition after heat treatment was determined by atomic absorption spectra.

Vapour-phase oxidative carbonylation of methanol

The vapour-phase DMC synthesis reaction by oxidative carbonization of methanol with carbon monoxide and oxygen was investigated using a continuous flow system in a fixed bed reactor. The reactor was made of a stainless steel tube having an inner diameter of 10 mm and a length of 40 cm. About 0.25 g (~0.3 mL) catalyst mixed with quartz grain was packed into the tubular reactor. Methanol was introduced with a syringe pump by 0.056 mL/min into the pre-heater, where it was vaporized. It then entered the reactor together with carbon monoxide and oxygen. An electronic mass flow controller was used to control the flow rate of carbon monoxide and oxygen. The reaction products leaving the reactor passed through an ice-water cooling trap and were separated by a gas-liquid separator. The liquid products were then weighed and measured with a flame ionization detector (FID) equipped with a 30 m capillary column of fused silica containing RSL 160 liquid phases for the separation of methanol, DMC, methyl formate (MF) and dimethoxy methane (DMM). The uncondensed gas products (O_2, CO_2 and CO) were introduced to the GC through an on-line six-way valve and analyzed by TCD detection with a TDX-01 packed column. The error margin of the GC was 1–2%. Traces of CO_2 were detected in the product, and thus the CO_2 was not taken into consideration when calculating the mass balance. MF and DMM were the only significant byproducts detected. The carbon balance of the experiments was all in range of 95-99%[40].

The reaction and side reactions were listed in Eqns (1)–(3):

$$2CH_3OH + CO + 1/2O_2 \rightarrow CH_3OCOOCH_3 + H_2O \quad ...(1)$$

$$2CH_3OH + O_2 \rightarrow HCOOCH_3 + 2H_2O \quad ...(2)$$

$$3CH_3OH + 1/2O_2 \rightarrow CH_3OCH_2OCH_3 + 2H_2O \quad ...(3)$$

Methanol conversion (C_{MeOH}), the selectivities of DMC, MF, and DMM (S_{DMC}, S_{MF} and S_{DMM}) as well as the space–time yield of DMC (STY_{DMC}) were calculated from the stoichiometry of Equations (4)–(8):

$$C_{MeOH} = \frac{3*n_{DMM} + 2*n_{MF} + 2*n_{DMC}}{3*n_{DMM} + 2*n_{MF} + 2*n_{DMC} + n_{MeOH}} \times 100\% \quad ...(4)$$

$$S_{DMC} = \frac{2*n_{DMC}}{2*n_{DMC} + 3*n_{DMM} + 2*n_{MF}} \times 100\% \quad ...(5)$$

$$S_{MF} = \frac{2*n_{MF}}{2*n_{DMC}+3*n_{DMM}+2*n_{MF}} \times 100\% \quad ...(6)$$

$$S_{DMM} = \frac{3*n_{DMM}}{2*n_{DMC}+3*n_{DMM}+2*n_{MF}} \times 100\% \quad ...(7)$$

$$STY = \frac{m_{DMC}}{m_{cat}*t} = \frac{V_{MeOH}*t*_{MeOH}*C_{MeOH}*S_{DMC}*M_{DMC}}{2*M_{MeOH}} * \frac{1}{m_{cat}*t} \times 100\% \quad ...(8)$$

wherein，m_{DMC}：the mass of DMC (g);

m_{cat}：the mass of catalyst (g);

V_{MeOH}：the flow rate of MeOH (mL/min);

ρ_{MeOH}：the density of MeOH (g/mL);

t：reaction time (h)

n_X: the molar amount of X (X=DMC, DMM and MF) (mol)

Results and Discussion

Oxidative carbonylation of methanol

The catalytic activities of the carbon-supported copper catalysts with different promoters in the gas-phase oxidative carbonylation of methanol are shown in Table 1 and Table 2. It can be seen that there are no obvious difference in the DMC selectivity for the three catalysts, and they almost kept constant during the reaction. However, the MeOH conversion and STY of DMC start to increase, reach maximum values after 4 h, then start to decrease. The MeOH conversion, DMC selectivity and STY obtained on the Cu/AC catalyst are 3.4%, 81.5% and 412.3 $mg \cdot g^{-1} \cdot h^{-1}$, respectively. It can be seen that there is an obvious improvement in the catalytic activity after the addition of La or Zr promoters. For the LaCu/AC and ZrCu/AC catalysts, five sets of relevant experiments are conducted which kept better reproducibility, the MeOH conversion increases to the maximum of 4.0% and 4.7% and the STY of DMC reach 480.2 and 585.2 $mg \cdot g^{-1} \cdot h^{-1}$, respectively. These results show that addition of La or Zr promoters has a remarkable influence on the catalytic performance of carbon-supported copper catalysts in the DMC synthesis.

Characterization of catalysts

XRD

XRD measurements were carried out to analyze the status and crystal structure of the copper species present on the carbon support. Powder XRD patterns of Cu/AC, LaCu/AC and ZrCu/AC catalysts prepared in the microwave oven are shown in Fig. 1. In all cases, a

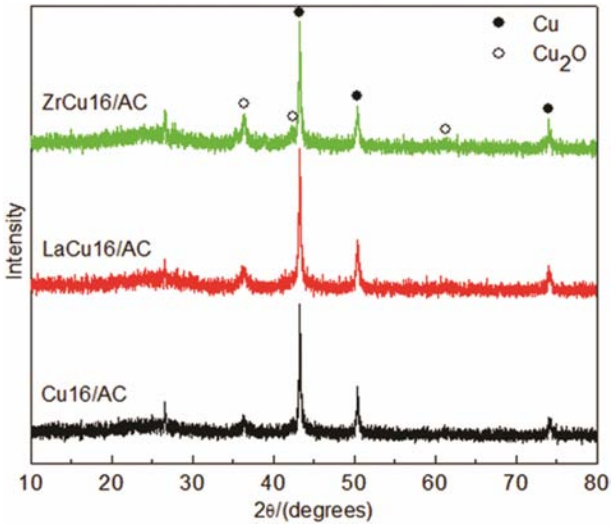

Fig. 1 — Powder XRD patterns of carbon-supported copper catalysts.

Table 1 — Catalytic results of Cu/AC and reproducibility for Cu-La/AC catalyst

NO.	Catalysts	$W_{cat.}$(g)	C_{MeOH}(%)	S_{DMC}(%)	S_{DMM}(%)	S_{MF}(%)	STY_{DMC}(mg/g·h)
1	Cu/AC	0.25	3.4	81.5	2.3	16.2	412.3
2	Cu-La/AC	0.25	3.9	94.8	0.6	4.6	465.8
3	Cu-La/AC	0.25	3.8	90.3	0.9	8.8	453.1
4	Cu-La/AC	0.25	3.3	86.6	1.7	11.7	429.9
5	Cu-La/AC	0.25	3.9	94.2	0.4	5.4	463.9
6	Cu-La/AC	0.25	4.0	95.7	0	4.3	480.2

Table 2 — Results for reproducibility of Cu-Zr/AC catalyst

NO.	Catalyst	$W_{cat.}$(g)	C_{MeOH}(%)	S_{DMC}(%)	S_{DMM}(%)	S_{MF}(%)	STY_{DMC}(mg/g·h)
1	Cu-Zr/AC	0.25	4.7	89.9	0.1	10.0	545.2
2	Cu-Zr/AC	0.25	4.6	87.2	0.4	12.4	533.6
3	Cu-Zr/AC	0.25	4.7	90.3	0	9.7	550.3
4	Cu-Zr/AC	0.25	4.5	84.2	0.7	15.1	523.1
5	Cu-Zr/AC	0.25	4.7	90.0	0.2	9.8	543.7

rather wide diffraction peak at 2θ=26.5°, corresponding to the graphite-C, can be observed. Strong diffraction lines, at 2θ=43.3°, 50.4°, and 74.1°, are observed in all three samples. These peaks are identified as the diffraction peaks of metallic copper (JCPDS No. 04-0836). In addition, a very small peak at 36.5° is also detected, which can be attributed to crystalline Cu_2O[41]. These results indicate that the copper species in these carbon-supported copper catalysts is mainly in the form of Cu^0. It is known that both Cu_2O and Cu^0 are formed as a consequence of the auto-reduction of the copper-containing compounds by the carbonaceous support[42]. It is also certain that copper-containing compounds can be quickly reduced to Cu_2O and Cu through microwave heating in a vacuum.

H_2-TPR

Figure 2 shows the results of TPR measurements on the catalyst Cu/AC, as well as the catalysts with promoters LaCu/AC and ZrCu/AC. It can be seen that all the catalysts produce three peaks and clearly reduced at three stages, 150~300°C, 300~450°C and 450~800°C, respectively. The peak positions and relative contributions of copper species with different

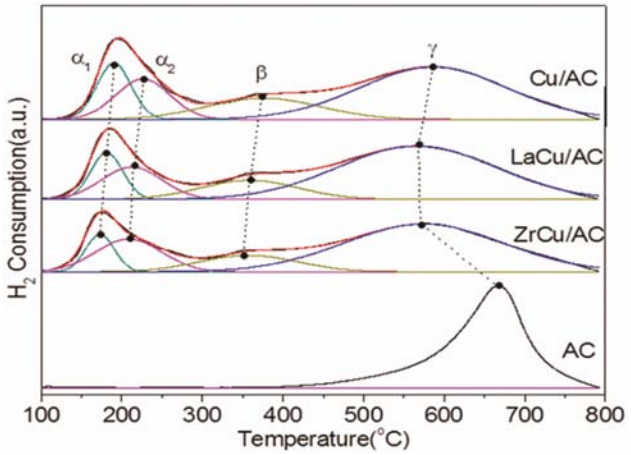

Fig. 2 — H_2-TPR profiles of carbon-supported copper catalysts.

valence states calculated from H_2-TPR profiles are listed in Table 3.

For the three catalysts, the first reduction peak can be regarded as two peaks denoted as α_1 and α_2. Since no diffraction peaks of crystalline CuO are observed in the XRD patterns, the α_1 peak must be related to the reduction of the well-dispersed CuO to Cu^0 (Ref. 43), while the α_2 peak corresponded to the reduction of Cu^{2+} immobilized onto the functional groups of active carbon[44]. The peak occurred in the range of 300 to 450°C was denoted as β peak, which could be assigned to the reduction of isolated Cu^+ to Cu^0 (Ref. 45). The last peak (the γ peak) appeared from 450 to 800°C could be attributed to the gasification of active carbon[46], confirmed by the TPR of support as a blank test.

As shown in Table 3, the reduction peaks of the Cu species shift to lower temperature with the addition of La or Zr promoters, and the reduction peak area is greatly reduced. These findings indicate that the La and Zr promoters can enhance the reducibility of the copper species in the carbothermic reduction reaction[42,47]. It also can be seen that there is a significant increase in the content of Cu^0, while the amount of Cu^{2+} and Cu^+ species decreases, attributed to the addition of La and Zr. This result reveals that the addition of La and Zr promoters enhances the formation of metallic copper in the microwave heating of the carbon-supported copper catalysts.

XPS

Characterization of the oxidation state of the copper species present on the surface of the samples may be made by means of XPS by studying the shift of the BE of the Cu $2P_{3/2}$ photoelectron and Cu LMM Auger lines. Studies of many Cu^{2+} compounds have shown intense XPS shake-up satellite peaks at kinetic energies 8-9 eV lower than the Cu $2p_{1/2}$ and Cu $2p_{3/2}$ core level peaks. The intensity of these shake-up

Table 3 — Quantitative H_2-TPR results of Cu/AC catalysts with different promoters

Catalysts	Peaks			Total area	Concentrations [a]		
	α_1 Temperature (%)	α_2 Temperature (%)	β Temperature (%)		W_{Cu}^{2+} [b] mg (%)	W_{Cu}^{+} [c] mg (%)	W_{Cu}^{0} [d] mg (%)
Cu/AC	189.8(29.7)	225.9(33.6)	374.2(36.7)	102286.0	6.17(34.3)	3.65(20.3)	8.18(45.4)
LaCu/AC	180.1(28.3)	212. 9(36.6)	362.4(35.1)	100111.4	5.28(29.3)	2.95(16.4)	9.77(54.3)
ZrCu/AC	172.4(22.3)	209.4(44.5)	358.9(33.2)	83216.7	4.57(25.4)	2.37(13.2)	11.06(61.4)

[a]Total copper content: 18.0 mg.

[b]W_{Cu}^{2+} calculated from area of H_2 consumption of peaks α_1 and α_2.

[c]W_{Cu}^{+} calculated from area of H_2 consumption of peak β.

[d]$W_{Cu}^{0} = W_{Cu}^{Total} - W_{Cu}^{2+} - W_{Cu}^{+}$

satellites, caused by simultaneous 2p and 3d excitation, has been deemed a useful analytical tool for differentiating Cu^{2+} and Cu^{+} species in solids[47]. XPS spectra of the Cu 2p core regions, acquired from carbon-supported copper catalysts and appropriate curve fits, are shown in Fig. 3. The peak positions and relative contributions from these features in the spectrum are collected in Table 3 and Table 4. In all cases the peak fit of the Cu $2p_{3/2}$ core level reveals the presence of two Cu species at different BE; the lower, at ~932.5 eV, corresponds either to Cu^{+} or Cu^{0} while the higher, at ~934.3 eV, is characteristic for divalent, paramagnetic Cu^{2+} ions. The satellite structure in the spectra of the carbon-supported copper catalysts is consistent with this conclusion.

The chemical states of Cu^{+} and Cu^{0} are not distinguishable on the basis of their Cu $2P_{3/2}$ Bes, but the differences in the Auger parameters are significant[49]. The modified Auger parameter α', which represents the summation of the kinetic energy (KE) of the Cu LMM Auger electron and the BE of the Cu $2p_{3/2}$ photoelectron, was therefore employed to distinguish between the Cu^{+} and Cu^{0} species.

Figure 4 shows Cu LMM Auger spectra of carbon-supported copper catalysts. In all cases, two peaks appear, at ~912.7 eV and ~916.7 eV, and the α' values are 1845.2 and 1849.2eV, respectively. It is reported that the α' values of Cu^{1+} and Cu^{0} are 1849 eV and 1851 eV, respectively. Also, when copper (with +2, +1, 0 valence) is in the highly dispersed state and in intimate contact with the supports, α' can be 2-3 eV lower than the bulk values[50]. This result indicates that the copper species associated with the BE ~912.7 eV and ~916.7 eV should be assigned to Cu^{1+} and Cu^{0}, respectively. In addition, Cu^{0} is the main copper species on the surface of the carbon-supported copper catalysts. This is in accordance with the results of the XRD analysis.

The surface atomic concentration of copper and other elements of carbon-supported copper catalysts calculated from the XPS data is also summarized in Table 5. It can be seen that there is a marked increase in the concentration of Cu when La or Zr was added to the catalysts. The surface atomic concentration of copper is 1.9%, 1.9%, and 2.2% for samples Cu/AC, LaCu/AC and ZrCu/AC, respectively. The XPS data show that, apart from Cu^{0}, a very *small quantity* of Cu^{2+} and Cu^{1+} species are also present on the surface of the carbon-supported copper catalysts. Peak fits of the XPS Cu $2p_{3/2}$ and Cu LMM Auger spectra of the carbon-supported copper catalysts are given in Table 4. It is observed that the concentration of Cu^{0} species increases with the addition of La or Zr in the catalysts. With the addition of La and Zr, the surface concentration of Cu^{0} increases from 1.0% to 1.1% and

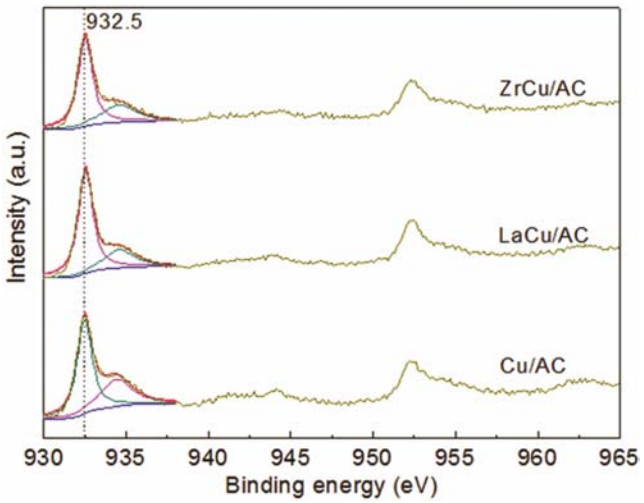

Fig. 3 — The Cu 2p core-level XPS spectra of carbon-supported copper catalysts.

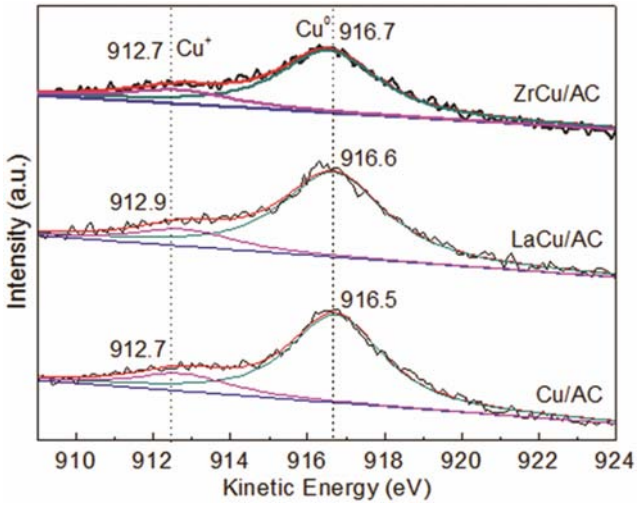

Fig. 4—Cu LMM Auger spectra of carbon-supported copper catalysts.

Table 4 — Peak fit of the XPS Cu $2p_{3/2}$ and Cu LMM Auger spectra of carbon-supported copper catalysts

Catalysts	BE(eV)		KE(eV)		Surface Cu (%)	Cu^{0} (%)
	Cu^{2+}	$Cu^{1+}+Cu^{0}$	Cu^{1+}	Cu^{0}		
Cu/AC	934.4(37%)	932.5(63%)	912.7(17%)	916.7(83%)	1.9	1.0
LaCu/AC	934.6(26%)	932.5(74%)	912.9(20%)	916.6(80%)	1.9	1.1
ZrCu/AC	934.5(31%)	932.5(69%)	912.7(20%)	916.5(80%)	2.2	1.2

Table 5 — Elemental chemical analysis in the near surface region of carbon-supported copper catalysts

Sample	Atom concentration (%)				
	C_{1s}	O_{2s}	La_{3d}	Zr_{3d}	Cu_{2p}
Cu/AC	83.1	15.0	-	-	1.9
LaCu/AC	83.3	14.6	0.2	-	1.9
ZrCu/AC	78.1	18.2	-	1.5	2.2

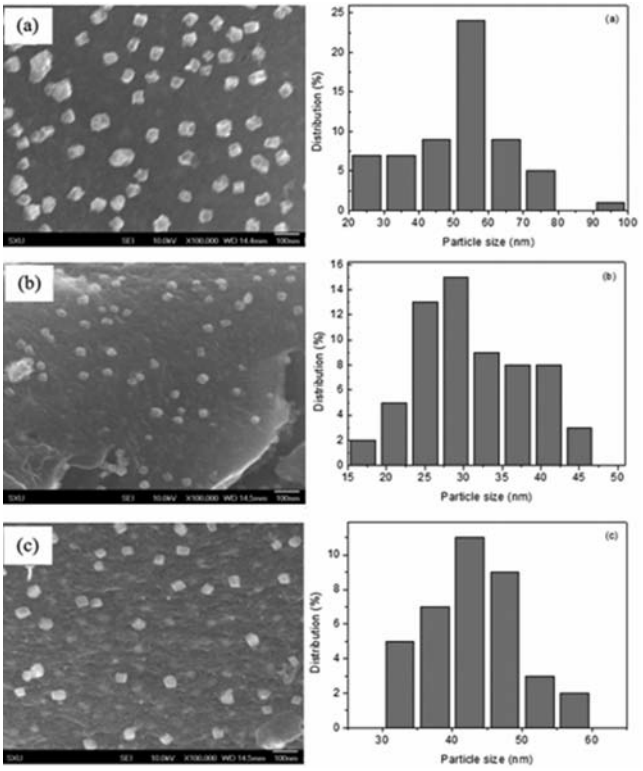

Fig. 5 — SEM images (left) and corresponding size distribution (right) of carbon-supported copper catalysts: (a) Cu/AC, (b) LaCu/AC and (c) ZrCu/AC.

1.2%, respectively. This finding demonstrates that the addition of La and Zr to carbon-supported copper catalysts contributes to the enrichment of the Cu species on the surface of the support. Moreover, it also further confirms that the addition of La or Zr favors the auto-reduction of copper precursors to metallic copper, which is thought to be the most active phase for the synthesis of DMC.

SEM

The external morphology of the carbon-supported copper catalysts is revealed by SEM. Figure 5 shows the SEM photomicrographs and histograms of the Cu particle size distributions for the carbon-supported copper catalysts. Figure 5(a) shows that the Cu particles prepared without addition of promoters exhibit a large average size of 52 nm and a broad size distribution, ranging from ~20 to 80 nm. A great many isolated metallic copper particles were regularly dispersed on the surface of the carbon support.

However, the Cu particles are not well dispersed on the carbon support due to their apparent tendency to agglomerate. Figures 5(b) and (c) show that the Cu nanoparticles become smaller and more uniform when a small amount of promoter is added to the catalyst. The average size of the Cu particles decreases to 31 and 42 nm, respectively for the catalysts with the addition of La and Zr promoters. In addition, as shown in Figs 5(b) and (c), the Cu nanoparticles are only rarely agglomerated and are generally highly dispersed on the carbon surface after addition of the appropriate amount of La or Zr promoter. Therefore, it is evident that La and Zr are good promoters for preparing small and uniform Cu nanoparticles, highly dispersed on a carbon support, using microwave assisted preparation. The reduction in the size of active phase particles resulting from the addition of La or Zr could be one of the reasons for the improvement of the catalyst activity and selectivity[51].

Conclusion

The microwave heating technique has been shown to be a very promosing method for the preparation of highly dispersed carbon–supported copper catalysts. It is found that the addition of La or Zr promoters has a significant influence on the size and dispersion of Cu nanoparticles on the surface of the carbon support and the catalytic performance of Cu/AC catalysts for the oxidative carbonylation of methanol to DMC. With the addition of La or Zr, there is a sharp decrease in the size of the Cu nanoparticles. The distribution range of the Cu nanoparticles is narrowed from 10~100 nm to 10~60 nm, and the catalytic activity of Cu/AC catalysts for the synthesis of DMC is greatly improved which exhibted the promising STY_{DMC} of 480.2 and 585.2 $mg \cdot g^{-1} \cdot h^{-1}$, respectively. Meanwhile, the S_{DMC} reached 95.7% and 90.3% and higher C_{CH_3OH} of approximately 4.0% and 4.7% achieved surprisingly, even after five sets of relevant experiments. It is evident that the addition of La or Zr promotes the auto-reduction of copper precursors to metallic copper and limits the aggregation of the Cu nanoparticles, consequently improving the catalytic performance of these Cu/AC catalysts.

Acknowledgements

This work has been supported by a grant from the National Natural Science Foundation of China (21376159 and 21276169).

References

1 Pacheco M A & Marshall C L, *Energy Fuels*, 11 (1997) 2.
2 Peng W C, Zhao N, Xiao F K, Wei W & Sun Y H, *Pure Appl Chem*, 84 (2012) 603.
3 Tomishige K, Sakaihori T, Sakai S I & Fujimoto K, *Appl Catal A: Gen*, 181 (1999) 95.
4 Wang Y J, Zhao X Q, Yuan B G, Zhang B C & Cong J S, *Appl Catal A: Gen*, 171 (1998) 255.
5 Han M S, Lee B G, Suh I, Kim H S, Ahn B S & Hong S I, *J Mol Catal A: Chem*, 170 (2001) 225.
6 Yang P, Cao Y, Hu J C, Dai W L & Fan K N, *Appl Catal A: Gen*, 241 (2003) 363.
7 Yuan Y Z, Cao W & Weng W Z, *J Catal*, 228 (2004) 311.
8 King S T, *J Catal*, 161 (1996) 530.
9 Li Z, Xie K C & Slade R C T, *Appl Catal A: Gen*, 205 (2001) 85.
10 Anderson S A & Root T W, *J Catal*, 217 (2003) 396.
11 Zhang Y H, Drake I J, Briggs D N & Bell A T, *J Catal*, 244 (2006) 219.
12 Shen Y L, Meng Q S, Huang S Y, Wang S P, Gong J L & Ma X B, *RSC Adv*, 2 (2012) 7109.
13 Zhang Y H & Bell A T, *J Catal*, 255 (2008) 153.
14 Zheng X B & Bell A T, *J Phys Chem C*, 112 (2008) 5043.
15 Richter M, Fait M J G, Eckelt R, Schneider M, Radnik J, Heidemann D & Fricke R, *J Catal*, 245 (2007) 11.
16 Richter M, Fait M J G, Eckelt R, Schreier E, Schneider M, Pohl M M & Fricke R, *Appl Catal B: Environ*, 73 (2007) 269.
17 Li Z, Wen C M, Wang R Y, Zheng H Y & Xie K C, *Chem J Chinese U*, 30 (2009) 2024.
18 Wang R Y, Li Z, Zheng H Y & Xie K C, *Chinese J Catal*, 31 (2010) 851.
19 Dong Y Y, Huang S Y, Wang S P, Zhao Y J, Gong J L & Ma X B, *Chem Cat Chem*, 5 (2013) 2174.
20 Shen Y L, Meng Q S, Huang S Y, Gong J L & Ma X B, *Phys Chem Chem Phys*, 15 (2013) 13116.
21 Ren J, Guo C J, Yang L L & Li Z, *Chinese J Catal*, 34 (2013) 1734.
22 Ren J, Wang W, Wang D L, Zuo Z J, Lin J Y & Li Z, *Appl Catal A: Gen*, 472 (2014) 47.
23 Hao P, Ren J, Yang L, Qin Z, Lin J, & Li Z, *Chem Eng J*, 283 (2016) 1295.
24 Armadi I S, Wang Z L, Green T C, Henglein A & El-Sayed M A, *Science*, 272 (1996) 1924.
25 Ren J, Yang L, Wang DL, Qin ZF, Pei YL, Lin JY, & Li Z, *Asian J Chem*, 27 (2015) 1381.
26 Ren J, Wang DL, Pei YL, Qin ZF, Lin JY, & Li Z, *Chem J Chinese* U, 34 (2013) 2594.
27 Ren J, Ren M, Wang DL, Lin JY, & Li Z, *J Therm Anal Calorim*, 120 (2015) 1929.
28 Zhang B S, Ni X J, Zhang W, Shao L D, Zhang Q, Girgsdies F, Liang C H, Schlogl R & Su D S, *Chem Commun*, 47 (2011) 10716.
29 Baghbanzadeh M, Carbone L, Cozzoli P D & Kappe C O, *Angew Chem Int Ed*, 50 (2011) 11312.
30 Cross H E, Parkes G & Brown D R, *Appl Catal A,* 429-430 (2012) 24
31 Antonetti C, Oubenali M, Galletti A M R, Serpb P & Vannucci G, *Appl Catal A,* 421-422 (2012) 99.
32 Li Z, Yan S W & Fan H, *Fuel*, 106 (2013) 178.
33 Rao J, Vaidhyanathan B, Ganguli M & Ramakrishnan P A, *Chem Mater*, 11 (1999) 882.
34 Wu G S, Ren J & Sun Y H, *J Fuel Chem Techol*, 27 (2011) 472 (In Chinese) .
35 Gao Z H, Huang W, Yin L H & Xie K C, *Chinese J Catal*, 32 (2011) 309.
36 Lin M G, Yang C, Wu G S, Wei W, Li W H, Shan Y K, Sun Y H & He M Y, *Chinese J Catal*, 25 (2004) 591.
37 Sun K P, Lu W W, Qiu F Y & Xu X L, *J Mol Catal A: Chem*, 17 (2003) 168-172. (In Chinese)
38 Li Z, Liu Y, Fan H & Zheng H Y, *Chinese J Inorg Chem*, 26 (2010) 1245.
39 Gao Z H, Huang W, Wang J Y, Yin L H & Xie K C, *Acta Chim Sinica*, 66 (2008) 295.
40 Yan B, Huang S, Wang S & Ma X, *Chem Cat Chem*, 6 (2014) 2671.
41 Xiang J Y, Tu J P, Yuan Y F, Huang X H, Zhou Y & Zhang L, *Electrochem Commun*, 11 (2009) 262.
42 Samouhos M, Hutcheon R & Paspaliaris I, *Miner Eng*, 24 (2011) 903.
43 Zhang B, Hui S G, Zhang S H, Ji Y, Li W & Fang D Y, *J Nat Gas Chem*, 21(2012)563.
44 Figueiredo J L, *J Mater Chem A*, 1 (2013) 9351.
45 Kim S C & Shim W G, *Appl Catal B: Gen, Environ*, 79 (2008) 149.
46 Bian J, Xiao M, Wang S J, Lu Y X & Meng Y Z, *Catal Commun*, 10 (2009) 1142.
47 Vennerberg D, Quirino R & Kessler M R, *Adv Eng Mater*, 15 (2013)366.
48 Sun K P, Lu W W, Qiu F Y, Liu S W & Xu X L, *Appl Catal A: Gen*, 252 (2003) 243.
49 Kohler M A, Curry-Hyde H E, Sexton B A & Cant N W, *J Catal*, 108 (1987) 323.
50 Chen L F, Guo P J, Qiao M H, Yan S R, Li H X, Shen W, Xu X L & Fan K N, *J Catal*, 257 (2008) 72.
51 Sajjadi S M, Haghighi M, Eslami A A & Rahmani F, *J Sol-Gel Sci Technol*, 67 (2013) 601